APPLIED AND ENVIRONMENTAL MICROBIOLOGY, Dec. 2006, p. 7701–7710 Vol. 72, No. 12
0099-2240/06/$08.00+0 doi:10.1128/AEM.01294-06

Escherichia coli Biofilms Formed under Low-Shear Modeled Microgravity in a Ground-Based System▽†

S. V. Lynch,[1]‡ K. Mukundakrishnan,[3] M. R. Benoit,[1] P. S. Ayyaswamy,[2] and A. Matin[1]*

Department of Microbiology and Immunology, Sherman Fairchild Science Building, Stanford University School of Medicine, 299 Campus Drive, Stanford, California 94305[1]; Department of Mechanical Engineering and Applied Mechanics, School of Engineering and Applied Science, University of Pennsylvania, Philadelphia, Pennsylvania 19104-6315[2]; and Department of Anesthesiology and Critical Care, University of Pennsylvania Medical Center, Philadelphia, Pennsylvania 19104[3]

Received 24 March 2006/Accepted 25 September 2006

Bacterial biofilms cause chronic diseases that are difficult to control. Since biofilm formation in space is well documented and planktonic cells become more resistant and virulent under modeled microgravity, it is important to determine the effect of this gravity condition on biofilms. Inclusion of glass microcarrier beads of appropriate dimensions and density with medium and inoculum, in vessels specially designed to permit ground-based investigations into aspects of low-shear modeled microgravity (LSMMG), facilitated these studies. Mathematical modeling of microcarrier behavior based on experimental conditions demonstrated that they satisfied the criteria for LSMMG conditions. Experimental observations confirmed that the microcarrier trajectory in the LSMMG vessel concurred with the predicted model. At 24 h, the LSMMG *Escherichia coli* biofilms were thicker than their normal-gravity counterparts and exhibited increased resistance to the general stressors salt and ethanol and to two antibiotics (penicillin and chloramphenicol). Biofilms of a mutant of *E. coli*, deficient in σ^s, were impaired in developing LSMMG-conferred resistance to the general stressors but not to the antibiotics, indicating two separate pathways of LSMMG-conferred resistance.

Bacteria colonize diverse ecological habitats where they can exist as single free-living (planktonic) cells or as communities encased in an exopolysaccharide and/or other matrix, referred to as biofilms. It is now clear that biofilm formation is part of the normal growth cycle of most bacteria (9, 10) and that, in the biofilm phase, bacteria exhibit greater resistance to a variety of stresses; these stresses include high salt, oxidizing agents, and low pH (referred to as "general" stressors [17]), as well as antibiotics used in treating common infections (9, 10). Thus, diseases in which biofilms play a major role (e.g., endocarditis, cystitis, and otitis media) tend to be chronic and difficult to treat.

Bacterial biofilms can also proliferate on board spacecraft. The now decommissioned MIR space station was heavily colonized by microbial biofilms, which caused extensive corrosion and blocked its water purification system (34). In-flight experiments have further confirmed that bacteria readily form biofilms during spaceflight (20). A unique stress encountered in this environment is diminished gravity (termed "microgravity"). We and others have shown that planktonic bacteria become more resistant and virulent when cultivated in ground-based systems that simulate aspects of microgravity. This resistance evidently has a unique molecular and biochemical basis (15, 37). Given these findings, we hypothesized that bacterial biofilms grown under modeled microgravity conditions may also exhibit altered characteristics.

Given the constraints on equipment and astronaut time, a thorough experimental examination of this hypothesis in space is difficult (16, 18). For significant progress, ground-based systems for biofilm cultivation under modeled microgravity conditions are necessary. We describe here such a system, involving the use of glass microcarriers in high-aspect-ratio vessels (HARVs) (15), and provide confirmation of its validity by mathematical analysis. Further, we discuss some of the characteristics of *Escherichia coli* biofilms grown under low-shear modeled microgravity (LSMMG). To our knowledge, this is the first report of ground-based studies of bacterial biofilms cultured under LSMMG.

MATERIALS AND METHODS

Mathematical modeling of microcarrier behavior in HARV system. Modeling was performed to calculate the expected microcarrier trajectory in a HARV rotating about a horizontal axis (LSMMG) and to ascertain the final location of the microcarrier under each condition. Equations used to model fluid flow, particle translation, rotation, and shear stress experienced by the bacteria cultured on the surface of microcarriers are presented in the supplemental material.

Bacterial strains. *E. coli* AMS6 (a K-12 derivative) and AMS150, an isogenic *rpoS* mutant strain deficient in σ^s, from our laboratory collection (30) were used in the present study. For visualization by confocal microscopy, both strains were transformed with pAD123 (obtained from the *Bacillus* Genetic Stock Center [www.bgsc.org] [7]), which constitutively expresses green fluorescent protein (GFP). These strains are referred to as AMS6(pAD123) and AMS150(pAD123), respectively. Luria-Bertani broth was used for all cultures; ampicillin (100 μg ml^{-1}) was added to cultures of strains containing pAD123.

Biofilm cultivation under LSMMG and biofilm visualization. An overnight culture of the desired fluorescent strain [either AMS6(pAD123) or AMS150(pAD123)] was diluted in fresh Luria-Bertani broth (A_{660} = 0.1), and 5

* Corresponding author. Mailing address: Department of Microbiology and Immunology, Sherman Fairchild Science Building, Stanford University School of Medicine, 299 Campus Drive, Stanford, CA 94305. Phone: (650) 725-4745. Fax: (650) 725-6757. E-mail: a.matin@stanford.edu.

† Supplemental material for this article may be found at http://aem.asm.org/.

‡ Present address: Department of Anesthesia and Perioperative Care, UCSF Medical School, 513 Parnassus Ave., San Francisco, CA 94143.

▽ Published ahead of print on 6 October 2006.

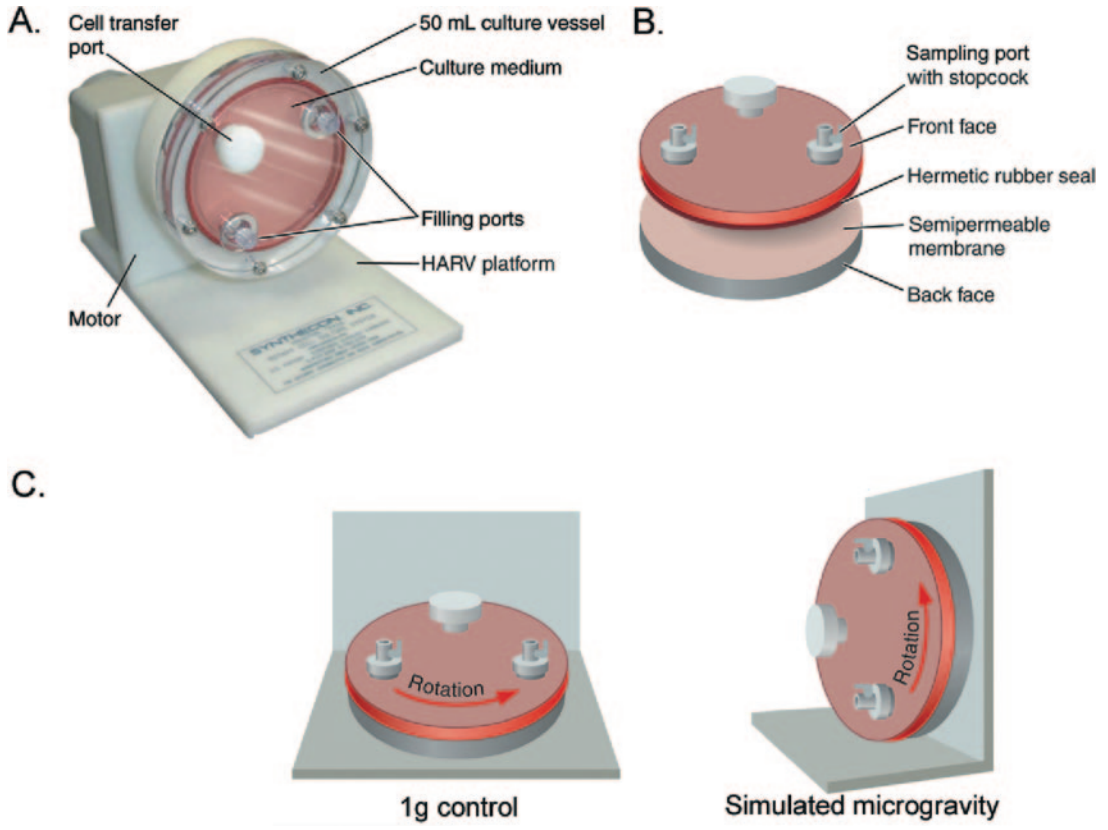

FIG. 1. (A) HARV system used to generate LSMMG conditions. (B) Individual constituents of the HARV vessel. (C) Orientation of HARV system to generate control (NG) or LSMMG conditions. (Adapted from Matin and Lynch [18].)

μg ml^{-1} sterile glass microcarrier beads (Sigma; 150 to 210 μm diameter; 1.02 g/cm^3) were added to the diluted culture. These microcarrier beads are ideal for these investigations since they are smaller and less dense than those successfully used previously for the suspension culture of anchorage-dependent mammalian cells (12, 14, 40). The mixture of beads, inoculum, and medium was used to fill a pair of HARVs. All bubbles were removed to eliminate turbulence in the HARV and ensure a low-shear environment. Vessels were rotated at 25 rpm either about a horizontal axis to generate LSMMG conditions or around a vertical axis, providing a normal gravity (NG) control (Fig. 1). Both vessels were incubated at 37°C for 24 h to permit sufficient time for biofilm formation on the surface of the glass beads. Aeration was achieved through a silicon semipermeable membrane at the back of the vessel.

To visualize the biofilms, a modified embedding method was used, using quick-setting polyacrylamide (4). Approximately 2.5 ml of medium containing microcarrier beads covered in biofilm was gently drawn into a 5-ml syringe containing 2.5 ml of a quick-setting polyacrylamide solution (5 ml of 200:1 acrylamide-bisacrylamide solution, 40 μl of TEMED [*N*,*N*,*N*′,*N*′-tetramethylethylenediamine], 500 μl of 1% ammonium persulfate). Syringes remained attached to the HARVs while the polyacrylamide set (approximately 30 s). The solidified polyacrylamide core was removed from the syringe and cut into thin sections. Several biofilm-containing beads close to the surface of the polyacrylamide slices were visualized with a Zeiss confocal scanning laser microscope, as previously described (33). Z-sections of several beads were collected and assembled by using Volocity3 software (Improvision, Massachusetts).

Stress tests. All stress tests were carried out on AMS6 and AMS150. Biofilms were cultured in the HARVs as described above. Stress solutions were added in separate experiments to a final concentration of 1 M NaCl, 7% ethanol, 500 μg of penicillin G ml^{-1}, or 4 μg of chloramphenicol ml^{-1}. A sample was gently removed (prior to and 1 h after addition of the specified stressor) and filtered to remove planktonic cells through a Millipore Swinnex-13 filter, housing an 8-μm-pore-size Whatman Nuclepore Track-Etch membrane. Biofilms on the beads were gently washed to ensure removal of all planktonic cells by passing 3 ml of sterile phosphate-buffered saline slowly through the membrane. Viability was determined by staining biofilms on the microcarriers with BacLight (Molecular Probes, Oregon). BacLight uses two dyes, propidium iodide and Syto9, which, due to differences in membrane integrity, stain nonviable cells red and stain viable cells green. Stained beads were examined with red and green filters by using an Olympus BX60 fluorescence microscope; the procedure permitted determination of viability of the surface layers of each biofilm and assessment of resistance differences.

Quantification of fluorescence. NIH freeware, ImageJ (available at http://rsb.info.nih.gov/ij/download.html), was used to quantify fluorescence from all experiments. Images were split into their red, green, and blue fluorescent components by using the "RGB split" function. Blue fluorescence readings were used as a control to ensure that fluorescence did not bleed through from the other channels (blue fluorescence readings were consistently 0). Integrated density readings (quantification of light emitted) of the green fluorescent images was measured and plotted to quantify biofilm formation. For viability studies that used BacLight staining, the integrated densities of both green and red fluorescence images were measured, and the percentage survival based on the mean initial number of viable cells (prestress) was calculated. *P* values were calculated by using the paired Student *t* test.

RESULTS

Mathematical modeling of microcarrier behavior in the HARV vessels. The numerical model considered a dilute distribution of microcarriers in the fluid-filled HARV since the distributed microcarrier density was calculated to be very small (10^{-6}). Given the diluteness of this mixture, interparticle interaction is assumed to be negligible, and hence the behavior of a single microcarrier was modeled. Particle trajectory for solid microcarrier beads was described by using direct numer-

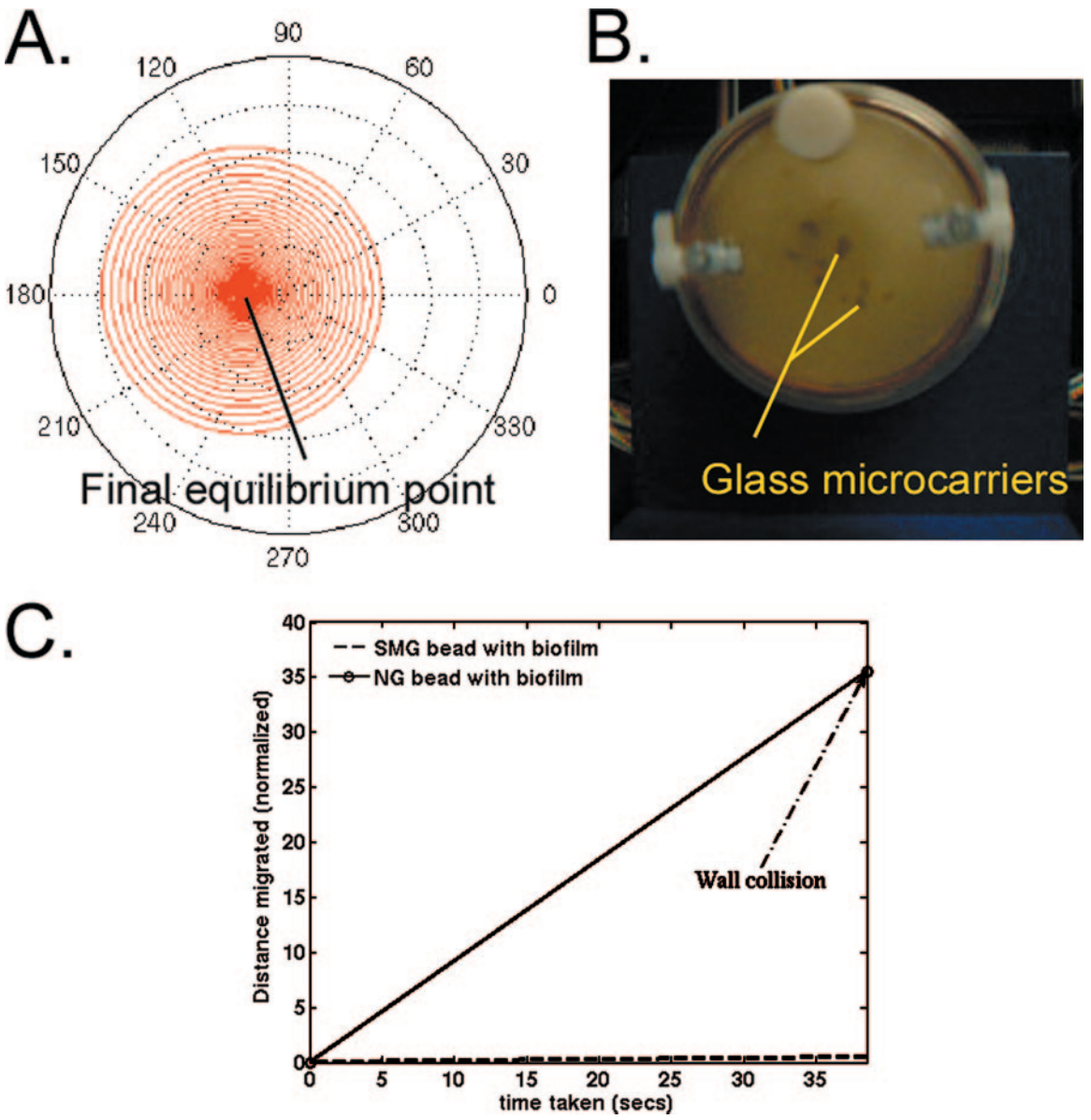

FIG. 2. (A) Numerically calculated trajectory (red trace) of a single microcarrier whose density is lighter than the culture medium as observed in a fluid-filled HARV rotated about a horizontal axis under experimental conditions. The particle spirals inward toward a fixed equilibrium point. (B) The observed behavior of microcarrier beads in a fluid-filled HARV under experimental conditions is in concordance with calculated behavior. Beads rotate in the center of the vessel (the image was captured 3 h postinoculation [see the supplemental material]). (C) Numerically predicted migration distance of a heavier bead (due to surface-attached biofilm) in NG and LSMMG bioreactors under identical culture conditions. The bead in the NG HARV quickly migrates downward along the axis of the HARV, whereas the bead in the LSMMG vessel migrates slowly radially outward toward the cylinder wall.

ical simulation techniques. Direct numerical simulation allows the description of fluid and microcarrier motion without making assumptions on the governing equations of motion describing the fluid flow and the particle trajectory.

Figure 2A illustrates the calculated trajectory in the fluid-filled HARV (using experimental parameters) of a representative microcarrier whose density is lower than the density of culture medium (representative of those used in biofilm experiments presented here) and the final equilibrium point reached by these beads under LSMMG conditions. The lighter particle eventually attains an equilibrium state at the center of its spiral trajectory and thus remains suspended for long periods of time. (Maintaining a colloidal suspension is an important feature of modeled microgravity.) The numerically predicted trajectory is in excellent agreement with the experimentally observed state (Fig. 2B; see Movie S1 in the supplemental material), in which the beads in the LSMMG HARV rotate in a gentle fluid orbit toward the center of the vessel where they remain suspended throughout the incubation.

Although the glass beads (without biofilms) were initially less dense than the fluid medium, we consistently observed settling of beads to the bottom of the NG HARV after 24 h of

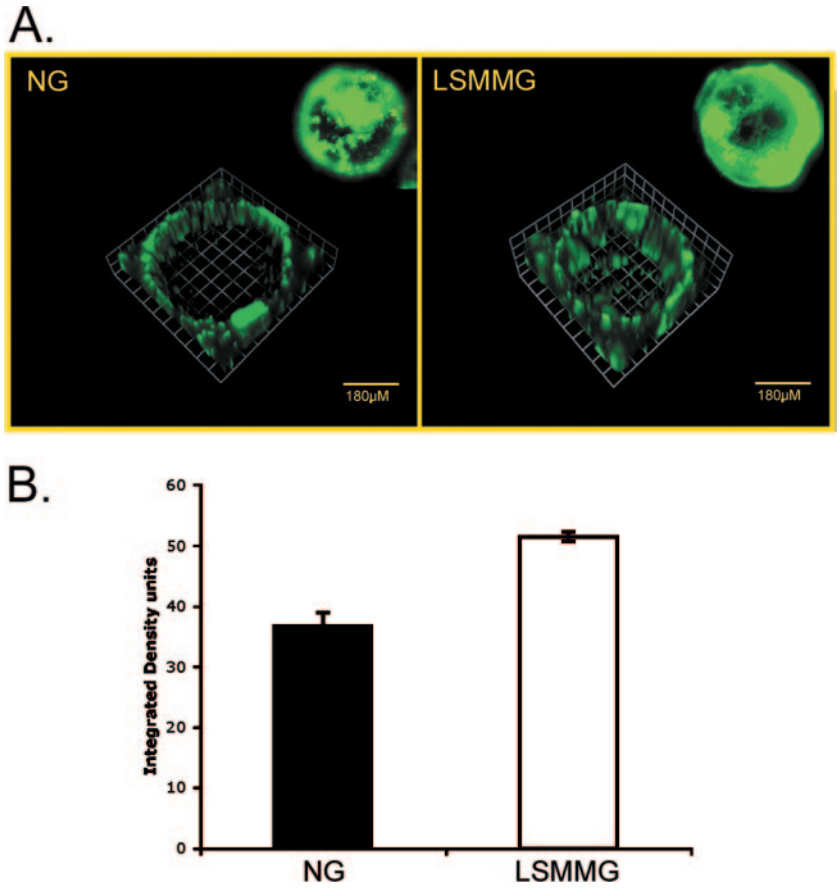

FIG. 3. (A) Z-stack assembly of NG and LSMMG biofilms at 24 h formed by AMS6(pAD123), constitutively expressing GFP, on microcarrier beads. The images in the upper right in each frame are representative x-y images of respective beads. (B) Quantification of GFP fluorescence of NG and LSMMG biofilms demonstrate significant differences ($P < 0.01$). The results represent an average of at least 10 beads from three independent experiments.

incubation. This phenomenon may be ascribed to the growth of surface-attached biofilms, which increase the apparent density of the microcarrier, making it heavier than the culture medium. Once beads reach the bottom of the HARV, no bead motion is predicted due to solid body rotation of the fluid. This behavior was consistently observed experimentally (see Movie S1 in the supplemental material). However, although the biofilm growth was denser on the LSMMG beads compared to the NG beads (Fig. 3 and 6), the LSMMG beads did not migrate radially outward during the 24-h incubation period. This may be explained by numerical simulations of the motion of a heavier bead (whose density is slightly greater than that of the culture medium) in an NG and an LSMMG bioreactor. Figure 2C illustrates the calculated normalized migration distance (migration distance was scaled by particle diameter) of NG and LSMMG beads under identical culture conditions. This demonstrates that the radial migration velocity of the LSMMG bead is much less than the axial migration of a NG bead. Due to the orientation of the NG bioreactor, the bead migrates downward along the axis of the HARV and, in the time taken for a NG bead (starting from the top of the bioreactor) to reach the base of the vessel, a similar bead under LSSMG conditions migrates a much shorter distance outward (approximately only half that of its own diameter). This difference in migration time arises mainly due to the differential effect of centrifugal and gravitational buoyancy (11, 22) in the two vessels. Thus, bead suspension time is much greater in the LSMMG HARV than in the NG HARV; Movie S1 in the supplemental material, taken after 24 h of incubation, demonstrates that the LSMMG beads remain suspended close to the center of the HARV.

Shear stress was calculated by using equation 14 (see Appendix S1 in the supplemental material). The maximum shear stress acting on a particle of density ($\rho_p = 1.02$ g/cm^3) under the experimental conditions described was ~0.02 dynes/cm^2 in the LSMMG vessel. In addition to the inwardly spiraling trajectory of a microcarrier in the LSMMG HARV as described above, the particle also rotates about its own axis. As the microcarrier rotates, so does the surface attached biofilm. The rotation rate of a microcarrier about its own axis was calculated (see equations in the supplemental material); a single orbit occurred approximately every 2.4 s (approximately equal to the rotation rate of the HARV).

***E. coli* forms more copious biofilms under LSMMG conditions.** AMS6(pAD123) biofilms were cultured on beads for 24 h in NG and LSMMG, embedded in quick-setting polyacrylamide, and visualized by confocal microscopy (as described in Materials and Methods). The resulting series of Z-sections

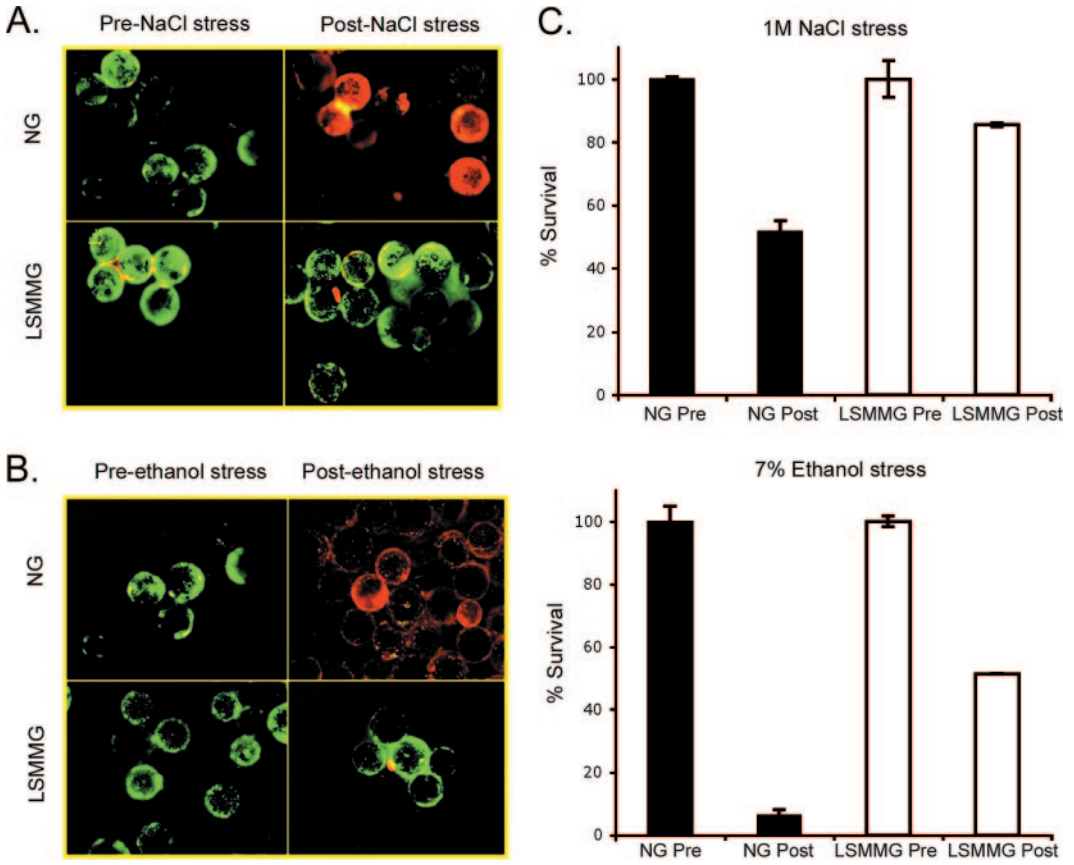

FIG. 4. (A and B) Representative images of *E. coli* AMS6 NG and LSMMG biofilms (stained with BacLight viability stain [green, viable; red, nonviable]) visualized pre- and post-NaCl (1 M) (A) or ethanol (7%) stress (B). (C) The percent survival was calculated on integrated density measurements of both red and green fluorescence under each condition. Significant differences in viability ($P < 0.017$ and $P < 0.000$ for NaCl and ethanol challenges, respectively) were seen. The results are representative of at least 10 beads from two independent experiments.

were assembled to provide a three-dimensional image of biofilm coverage on the upper hemisphere of the glass beads. Consistently, the LSMMG biofilms were denser than the NG biofilms, as indicated by visualization of the bead surfaces and fluorescence quantification (Fig. 3).

LSMMG-grown biofilms exhibit enhanced resistance. We and others have previously shown that LSMMG-grown planktonic cells exhibit enhanced resistance to a variety of stresses compared to their NG-grown counterparts (15, 23). To determine the effect of LSMMG on biofilm resistance, four separate stressors were investigated. Two of these were general stressors (NaCl and ethanol), and two were antibiotics with different modes of action (penicillin G, which inhibits peptidoglycan cross-linking, and chloramphenicol, which inhibits translation). Biofilms were grown in NG and LSMMG, exposed to each stress in situ for 1 h, stained by BacLight, and visualized. NG biofilms of AMS6 exposed to each of the above stresses exhibited mostly nonviable biomass (Fig. 4A and B and 5A). LSMMG biofilms exposed to the same stresses, in contrast, were predominantly viable (Fig. 4A and B and 5A). These observations were confirmed by quantification of the red and green fluorescence from multiple experiments as described in Materials and Methods (Fig. 4C and 5B). Thus, cultivation under LSMMG enhanced *E. coli* biofilm resistance to each of the general stressors and antibiotics tested.

Role of σ^s. σ^s plays a role in ground-based biofilm formation on Earth (1) and in the LSMMG-conferred increased resistance of stationary-phase planktonic cells to general stressors (15). We therefore investigated the effect of the loss of this sigma factor on biofilms formed under the two gravity conditions. Biofilms of the σ^s-deficient strain [AMS150(pAD123), constitutively expressing GFP] were consistently less dense under both NG and LSMMG conditions (Fig. 6), than those of the wild type (Fig. 3). However, biofilms formed by this strain under LSMMG remained more copious compared to NG-grown counterparts and exhibited the same extent of increased biofilm coverage as the wild-type LSMMG biofilm over NG (17 integrated density units; Fig. 3B and 6B). Thus, while σ^s deficiency impaired biofilm formation under both gravity conditions, it did not affect the stimulating influence of LSMMG on this phenomenon. It should be noted that AMS150 has the same growth rate as the isogenic wild-type strain (19).

Exposure of AMS150 biofilms cultured under NG or LSMMG conditions to either 1 M NaCl or 7% ethanol demonstrated a clear role for σ^s in increased general resistance of the LSMMG biofilms. Unlike the wild-type biofilms, those of the *rpoS* mutant failed to exhibit increased LSMMG-conferred resistance to these stresses (Fig. 7). However, the loss of σ^s did not affect LSMMG-conferred increased resistance to penicillin G or chloramphenicol. Beads containing the LSMMG-grown

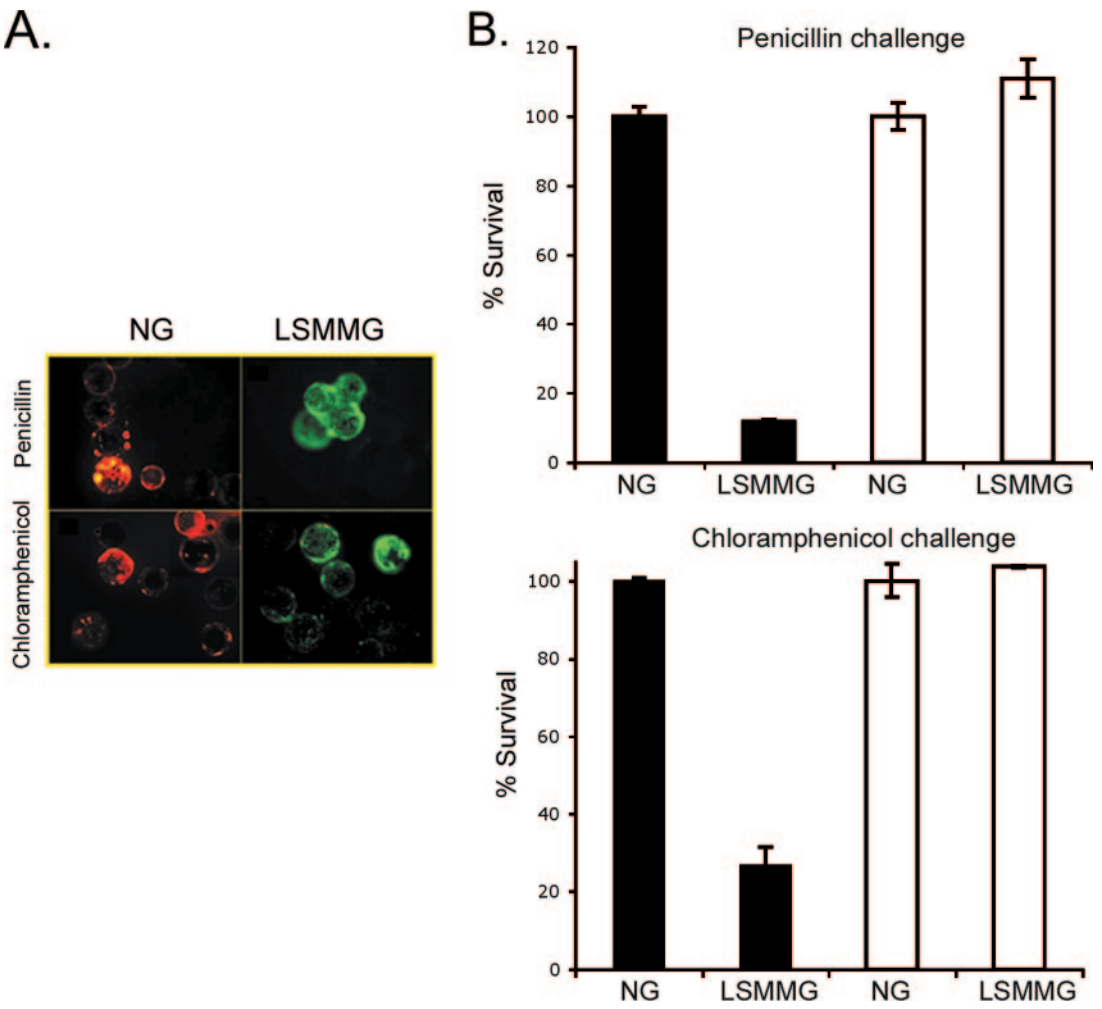

FIG. 5. (A) Biofilm viability of NG and LSMMG cultures after 1 h of exposure to penicillin G (500 μg ml^{-1}) and chloramphenicol (4 μg ml^{-1}), respectively. Pretreatment biofilms (image not shown) were predominantly viable for both cultures (similar to that shown in Fig. 5). (B) The percent survival was calculated on integrated density measurements of both red and green fluorescence under each condition. LSMMG biofilms were significantly more viable ($P < 0.000$ and $P < 0.001$ for penicillin and chloramphenicol challenges, respectively) than NG biofilms. The results are representative of at least 10 beads from two independent experiments.

biofilms of AMS150 exhibited mostly viable biomass after exposure to these antibiotics (Fig. 7), resembling the LSMMG-grown wild type in this respect (Fig. 5). The NG-grown biofilms of this mutant strain, like the wild type, were predominantly nonviable after these treatments (Fig. 4, 5, and 7).

DISCUSSION

Bacterial biofilms can pose serious health threats and have been shown to be significantly more resistant to antimicrobial and other stresses compared to planktonic cultures of the same organism (28, 29). Since it has been established that LSMMG makes planktonic bacteria more resistant and virulent (15, 23), it is important, for the safety of astronauts, to determine the effect of this environment on bacterial biofilms. In-flight experimentation in a microgravity environment is limited by technical difficulties and constraints on equipment availability and astronaut time. Thus, for a thorough investigation of the influence of aspects of this environment on microbial biofilms, ground-based systems are required for their cultivation under LSMMG.

HARVs, designed at the Johnson Space Center (Houston, Tex.), provide a model system for examining the effects of LSMMG in ground-based investigations (38, 39). In the horizontally rotated HARV, spherical objects of appropriate size and weight reach a steady-state terminal velocity at which the gravitational force is mitigated by equal and opposite hydrodynamic vectors, which include shear, centrifugal, and Coriolis forces. Studies with these systems have concentrated predominantly on planktonic cultures of *E. coli*, *Salmonella enterica* serovar *Typhimurium*, and *Pseudomonas aeruginosa* (8, 15, 23). The altered physiology of these bacteria when cultured under HARV LSMMG has correlated, by and large, with information from in-flight experiments, making HARVs a preferred system for ground-based investigations into the effect of aspects of microgravity on bacteria. However, while anchorage-dependent mammalian tissues have successfully been cultured using appropriate microcarriers for suspension culture in the

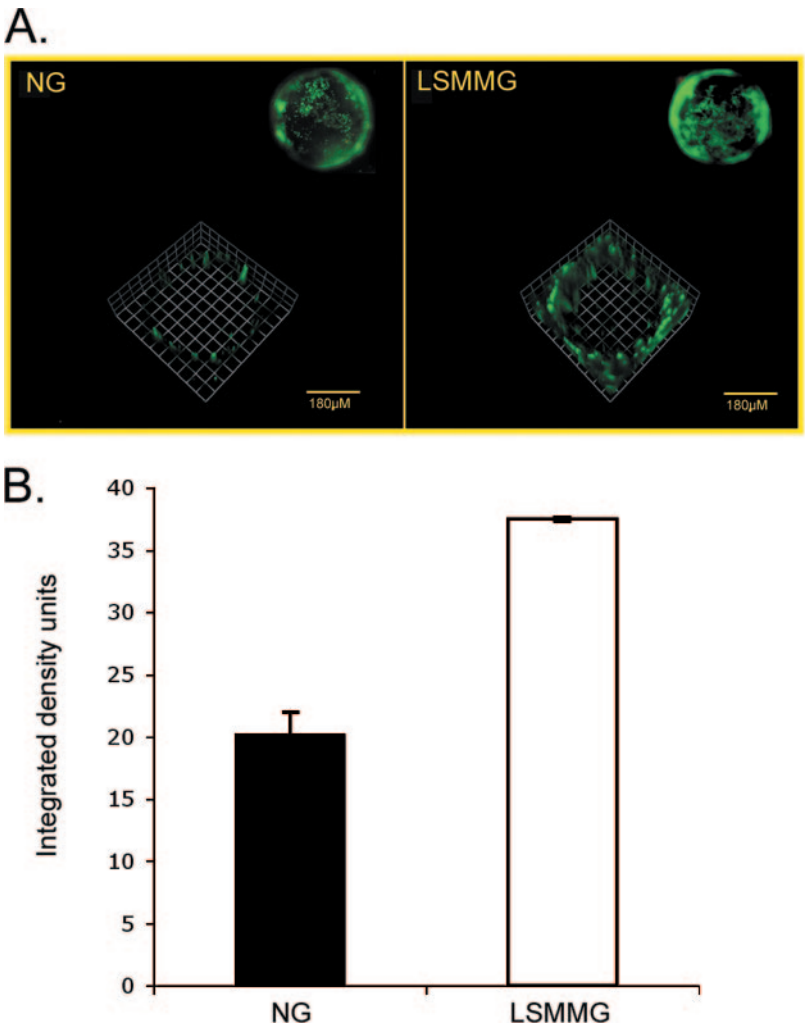

FIG. 6. (A) Z-stack assembly of NG and LSMMG biofilms at 24 h formed by AMS150(pAD123), constitutively expressing GFP, on microcarrier beads. The images in the upper right of each frame are representative x-y images of respective beads. (B) Quantification of GFP fluorescence of AMS150(pAD123) NG and LSMMG biofilms demonstrated significant difference in biomass ($P < 0.01$). The results represent an average of at least 10 beads from three independent experiments.

HARV system (12, 14, 40), this approach has not, to our knowledge, been used to cultivate microbial biofilms. The primary obstacle has been providing bacteria with a surface for biofilm formation that could be maintained under LSMMG. To overcome this, we included sterile glass microcarriers of appropriate size and density with bacterial inoculum and medium in the HARV system.

Microcarrier trajectory is dependent on its density and size, the density and viscosity of the culture medium, the rotational speed of the HARVs, the number of microcarriers used, and the bacterial inoculum (24, 27). The numerical model described here was based on the experimental parameters used. Calculations predicted that microcarriers in the LSMMG vessel should migrate toward a location near the center of the vessel. This was observed experimentally (see Movie S1 in the supplemental material). Further, the shear forces experienced by the microcarrier and its associated biofilm under experimental conditions were calculated and found to represent a very low shear force (0.02 dynes/cm^2). Suspension of the microcarrier and its surface-attached biofilm in the LSMMG vessel was maintained by balancing gravity-induced sedimentation with centrifugation (caused by the vessel rotation and fluid drag). The results of mathematical modeling based on the experimental conditions presented here imply that bacterial biofilms attached to microcarriers in the horizontally rotated HARV remain suspended in the fluid and experience very low shear, resembling aspects of a microgravity environment.

However, to successfully simulate aspects of microgravity, it is necessary that all of the following criteria be met: (i) microcarriers must be inert, and the shape of the microcarrier must be such as to minimize adverse flow effects; (ii) mass transport of nutrients and oxygen must be adequate; (iii) shear at the microcarrier/biofilm surface must be very low; (iv) microcarrier spin about its own axis must be calculated to assess the extent of gravitational vector neutralization due to rotation in the plane of gravity; and (v) collisions of microcarriers with each other and the vessel must be minimized (5). The microcarriers used in these experiments are inert glass beads and minimize

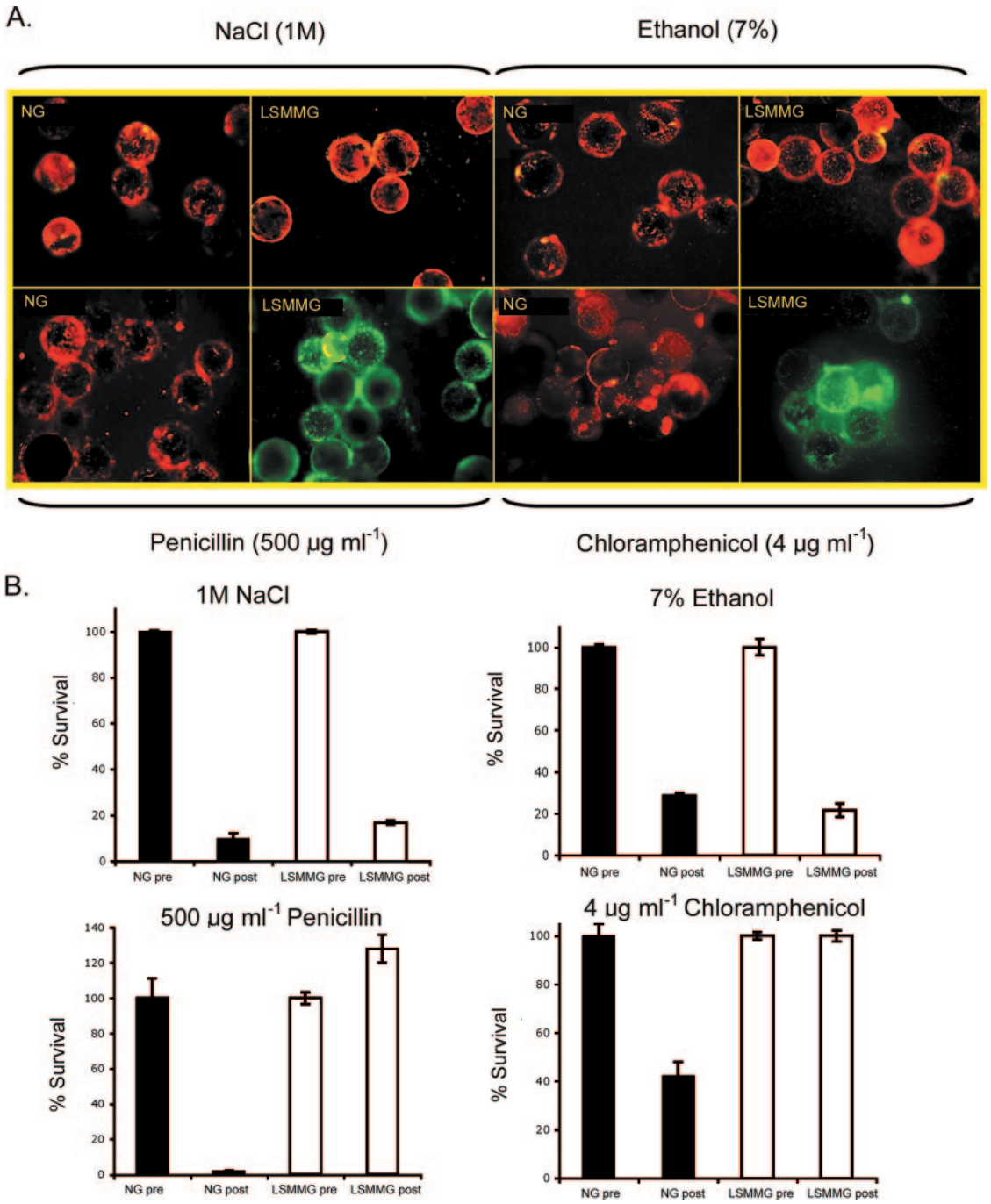

FIG. 7. (A) Stress resistance of AMS150 biofilms cultured under NG or LSMMG after exposure for 1 h to osmotic (1 M NaCl), ethanol (7%), penicillin (500 μg ml^{-1}), or chloramphenicol (4 μg ml^{-1}) stress. The results are representative of at least two separate experiments. (B) The respective percent survival of AMS150 grown under the same conditions and exposed to the same stresses as outlined above was calculated based on integrated density measurements of both red and green fluorescence under each condition. The results are representative of at least 10 beads from two independent experiments. The *P* values for poststress viability are as follows: 1 M NaCl, $P < 0.027$; 7% ethanol, $P < 0.085$; 500 μg of penicillin ml^{-1}, $P < 0.000$; 4 μg of chloramphenicol ml^{-1}, $P < 0.001$.

adverse flow effects due to their spherical shape, satisfying criterion i. Studies of mass transport of nutrients and oxygen in fluid-filled HARVs show that these processes occur efficiently under low-shear conditions in such vessels (2, 13, 32, 35), satisfying criterion ii. Calculation of shear forces based on experimental parameters confirmed that low shear conditions (calculated at 0.02 dyne) existed within the model system (criterion iii). Numerical modeling satisfied criterion iv, and the dilute nature of the microcarrier particle density distribution in the experimental system (calculated at 10^{-6}) predicts a low probability of collision between beads or the wall of the vessel, satisfying criterion v. We thus conclude that the model system

described here does provide conditions for cultivating bacterial biofilms under LSMMG conditions.

Beads in the LSMMG HARVs showed greater biofilm coverage than those incubated in the NG HARVs. Since beads in the latter sedimented, it could be argued that the relatively less coverage seen under NG conditions was due to a dearth of oxygen experienced by the sedimented biofilms. However, the HARV membrane has a large surface area (78.54 cm^2) and high oxygen permeability (5.2×10^{-4} ml cm^{-2} s^{-1}) and the vessel itself is narrow (width, 0.637 cm). Thus, the oxygen permeability rate in the HARV is likely to be as high as 0.041 ml s^{-1} (obtained by multiplying the oxygen permeability by the membrane area). At 1 atm pressure at 37°C, this corresponds to an availability of 1.6×10^{-6} mol-O_2 s^{-1}. *E. coli* typically consumes up to 15 mmol g^{-1} h^{-1} of oxygen (3). Thus, the HARV culture with 6×10^{10} total cells (or 0.06 g of cells, based on the maximal A_{660} readings we observed) can maximally consume 2.5×10^{-7} mol-O_2 s^{-1}, which is ~6-fold less than the O_2 availability rate, indicating the presence of sufficient oxygen throughout the HARV. Further, since aeration is through the membrane at the bottom of the HARV, the sedimented biofilms, if anything, will have more and not less oxygen available.

Another possibility is that the sedimented beads in the NG vessel, having attached to the membrane, may have been torn by the centrifugal forces, resulting in the disruption of the biofilm integrity. However, the HARVs were rotated at 25 rpm, generating a maximum centrifugal bead acceleration of 34.27 cm s^{-2} (at a maximum possible radial position of 5 cm), which is just 3.5% of the acceleration due to gravity. Furthermore, had the biofilms formed on the membrane and torn away from it or the beads during harvesting, they would have been seen on the 8-μm-pore-size filter after separation from the planktonic cells; there was no evidence of this. Taken together, these considerations indicate that the increased coverage of beads in the LSMMG HARV was due to their exposure to this shear and gravity condition.

Burkholderia cepacia biofilms formed on the space shuttle Atlantis had up to twofold higher viable counts compared to the controls on Earth (26). Thus, the biofilms formed under LSMMG in our system duplicated an aspect of actual microgravity biofilms, further indicating the suitability of our system for ground-based studies of biofilm biology in microgravity.

The comparative examination of NG and LSMMG biofilm resistance reported here demonstrates that LSMMG biofilms were resistant to concentrations of NaCl and ethanol that killed biofilms formed in the control (NG) vessels. These results, taken together with previous reports on enhanced resistance of planktonic LSMMG cultures (15), suggest that increased resistance to general stressors is a common characteristic of *E. coli* cultures in LSMMG regardless of their mode of growth. In addition, LSMMG also enhanced biofilm resistance to two antibiotics commonly used in treating infectious disease. It is noteworthy that each of these four stresses has a different mode of bacterial cell damage. High salt causes dehydration, ethanol disrupts the cell membrane, penicillin inhibits peptidoglycan synthesis, and chloramphenicol inhibits the synthesis of proteins. Thus, the changes induced by LSMMG in *E. coli* biofilms appear to have a blanket protective effect. It remains to be determined whether this effect is due to low shear, negation of microcarrier sedimentation, or a combination of both of these HARV characteristics. Regardless, these results highlight the potential increased threat that bacterial biofilms may pose during space exploration.

To gain insight into this comprehensive resistance mechanism, we examined the effect of loss of σ^s on *E. coli* biofilms grown under the LSMMG conditions; conventional Earth-based biofilms of strains carrying a mutation in this sigma factor exhibit altered characteristics (6, 25). *E. coli* AMS150, devoid of σ^s, formed less copious biofilms not only under NG, as expected, but also under LSMMG, indicating a role for this sigma factor also under the latter conditions. However, AMS150 biofilms cultured under LSMMG consistently displayed greater coverage of the microcarrier beads, suggesting that this environment has a stimulatory effect on biofilm formation independent of σ^s.

Under LSMMG, the mutant biofilm, unlike the wild-type biofilm, failed to induce increased resistance to general stressors, suggesting a role for σ^s in general stress response of *E. coli* biofilms in this environment. σ^s plays a role also in LSMMG-conferred resistance of stationary-phase planktonic cells to general stresses, although not in that exhibited by exponential-phase planktonic cells (15), suggesting a degree of similarity in the response of stationary-phase planktonic and biofilm cultures in LSMMG. This is consistent with recent reports that although biofilm state and planktonic growth represent different physiologies, the two have a greater similarity to each other than to planktonic exponential-phase cells (9, 31, 36). Interestingly, the loss of σ^s did not affect LSMMG-conferred increased resistance to the two antibiotics tested. Previously McLeod and Spector (21) demonstrated that starvation- and stationary-phase-associated polymyxin B resistance was independent of *rpoS* in *S. enterica* serovar Typhimurium. It appears that *rpoS*-independent antibiotic resistance exists also in *E. coli* biofilms cultured under LSMMG.

In addition to their pathogenic capacity, bacterial biofilms also have beneficial uses, for example, in microbe-based regenerative systems for wastewater treatment. These systems represent a viable alternative to physical and chemical methods in use today on the International Space Station. Thus, an investigation of the molecular physiology of biofilms will also enhance exploitation of their beneficial roles. The cultivation system we describe here therefore has multiple potential benefits.

ACKNOWLEDGMENTS

This research was supported by NASA grant NNA04CC51G. S.V.L. and M.R.B. were supported, in part, by a Deans Fellowship from the Stanford University School of Medicine and NIH training grant (T32) AI 07328 to the Department of Microbiology and Immunology, respectively.

REFERENCES

1. **Adams, J. L., and R. J. McLean.** 1999. Impact of *rpoS* deletion on *Escherichia coli* biofilms. Appl. Environ. Microbiol. **65:**4285–4287.
2. **Ayyaswamy, P. S., and K. Mukundakrishnan.** 18 October 2006, posting date. Optimal conditions for simulating microgravity employing NASA designed rotating wall vessels. Acta Astronautica [Online.] doi:10.1016/j.actaastro.2006.09.008.
3. **Calhoun, M. W., K. L. Oden, R. B. Gennis, M. J. de Mattos, and O. M. Neijssel.** 1993. Energetic efficiency of *Escherichia coli*: effects of mutations in components of the aerobic respiratory chain. J. Bacteriol. **175:**3020–3025.
4. **Christensen, B. B., C. Sternberg, J. B. Andersen, R. J. Palmer, A. T. Nielsen,**

M. Givskov, and S. Molin. 1999. Molecular tools for study of biofilm physiology. Methods Enzymol. **310:**20–42.
5. **Coimbra, C. F. M., and M. H. Kobayashi.** 2002. On the viscous motion of a small particle in a rotating cylinder. J. Fluid Mechanics **469:**257–286.
6. **Corona-Izquierdo, F. P., and J. Membrillo-Hernandez.** 2002. A mutation in *rpoS* enhances biofilm formation in *Escherichia coli* during exponential phase of growth. FEMS Microbiol. Lett. **211:**105–110.
7. **Dunn, A. K., and J. Handelsman.** 1999. A vector for promoter trapping in *Bacillus cereus*. Gene **226:**297–305.
8. **England, L. S., M. Gorzelak, and J. T. Trevors.** 2003. Growth and membrane polarization in *Pseudomonas aeruginosa* UG2 grown in randomized microgravity in a high aspect ratio vessel. Biochim. Biophys. Acta **1624:**76–80.
9. **Fux, C. A., J. W. Costerton, P. S. Stewart, and P. Stoodley.** 2005. Survival strategies of infectious biofilms. Trends Microbiol. **13:**34–40.
10. **Fux, C. A., P. Stoodley, L. Hall-Stoodley, and J. W. Costerton.** 2003. Bacterial biofilms: a diagnostic and therapeutic challenge. Expert Rev. Anti-Infect. Ther. **1:**667–683.
11. **Gao, H., P. S. Ayyaswamy, and P. Ducheyne.** 1997. Dynamics of a microcarrier particle in the simulated microgravity environment of a rotating-wall vessel. Microgravity Sci. Technol. **10:**154–165.
12. **Ikonomou, L., J. C. Drugmand, G. Bastin, Y. J. Schneider, and S. N. Agathos.** 2002. Microcarrier culture of lepidopteran cell lines: implications for growth and recombinant protein production. Biotechnol. Prog. **18:**1345–1355.
13. **Jessup, J. M., T. J. Goodwin, and G. F. Spaulding.** 1993. Prospects for use of microgravity-based bioreactors to study three-dimensional host-tumor interactions in human neoplasia. J. Cell. Biochem. **51:**290–300.
14. **Larina, O. N., L. A. Sidorenko, D. A. Moshkov, A. G. Pogorelov, L. L. Pavlik, A. V. Arutyunyan, I. A. Grivennikov, E. S. Manuilova, L. S. Inozemtseva, R. M. Umarkhodzhaev, and A. N. Pivkin.** 2002. Three-dimensional (3-D) structures formed by immortalized human fibroblast cells in simulated microgravity. J. Gravit. Physiol. **9:**P287–P288.
15. **Lynch, S. V., E. L. Brodie, and A. Matin.** 2004. Role and regulation of sigma S in general resistance conferred by low-shear simulated microgravity in *Escherichia coli*. J. Bacteriol. **186:**8207–8212.
16. **Lynch, S. V., and A. Matin.** 2005. Travails of microgravity: man and microbes in space. Biologist **52:**80–87.
17. **Matin, A.** 2000. Stress response in bacteria, vol. 6. John Wiley & Sons, Inc., New York, N.Y.
18. **Matin, A., and S. V. Lynch.** 2005. Investigating the threat of bacteria grown in space. ASM News **71:**235–240.
19. **McCann, M. P., J. P. Kidwell, and A. Matin.** 1991. The putative sigma factor KatF has a central role in development of starvation-mediated general resistance in *Escherichia coli*. J. Bacteriol. **173:**4188–4194.
20. **McLean, R. J., J. M. Cassanto, M. B. Barnes, and J. H. Koo.** 2001. Bacterial biofilm formation under microgravity conditions. FEMS Microbiol. Lett. **195:**115–119.
21. **McLeod, G. I., and M. P. Spector.** 1996. Starvation- and stationary-phase-induced resistance to the antimicrobial peptide polymyxin B in *Salmonella typhimurium* is RpoS (σ^S) independent and occurs through both *phoP*-dependent and -independent pathways. J. Bacteriol. **178:**3683–3688.
22. **Mukundakrishnan, K.** 2005. Fluid mechanics and mass transfer in rotating cylindrical vessels: a numerical and experimental study. Ph.D. thesis. University of Pennsylvania, Philadelphia.
23. **Nickerson, C. A., C. M. Ott, S. J. Mister, B. J. Morrow, L. Burns-Keliher, and D. L. Pierson.** 2000. Microgravity as a novel environmental signal affecting *Salmonella enterica* serovar *Typhimurium* virulence. Infect. Immun. **68:**3147–3152.
24. **Pollack, S. R., D. F. Meaney, E. M. Levine, M. Litt, and E. D. Johnston.** 2000. Numerical model and experimental validation of microcarrier motion in a rotating bioreactor. Tissue Eng. **6:**519–530.
25. **Prigent-Combaret, C. B. E., O. Vidal, A. Ambert, P. Lejeune, P. Landini, and C. Dorel.** 2001. Complex regulatory network controls initial adhesion and biofilm formation in *Escherichia coli* via regulation of the *csgD* gene. J. Bacteriol. **183:**7213–7223.
26. **Pyle, B. H., J. T. Lisle, M. A. Juergensmeyer, S. C. Broadaway, and G. A. McFeters.** 2001. Abstr. 31st International Conference on Environmental Systems, Orlando, Fla., abstr. 124P.
27. **Radin, S., P. Ducheyne, P. S. Ayyaswamy, and H. Gao.** 2001. Surface transformation of bioactive glass in bioreactors simulating microgravity conditions. I. Experimental study. Biotechnol. Bioeng. **75:**369–378.
28. **Schembri, M. A., K. Kjaergaard, and P. Klemm.** 2003. Global gene expression in *Escherichia coli* biofilms. Mol. Microbiol. **48:**253–267.
29. **Scher, K., U. Romling, and S. Yaron.** 2005. Effect of heat, acidification, and chlorination on *Salmonella enterica* serovar Typhimurium cells in a biofilm formed at the air-liquid interface. Appl. Environ. Microbiol. **71:**1163–1168.
30. **Schweder, T., K. -H. Lee, O. Lomovskaya, and A. Matin.** 1996. Regulation of *Escherichia coli* starvation sigma factor (σ^S) by ClpXP protease. J. Bacteriol. **178:**470–476.
31. **Spoering, A. L., and K. Lewis.** 2001. Biofilms and planktonic cells of *Pseudomonas aeruginosa* have similar resistance to killing by antimicrobials. J. Bacteriol. **183:**6746–6751.
32. **Stewards, R. P., T. J. Goodwin, and D. A. Wolf.** 1992. Cell culture for three-dimensional modeling in rotating-wall vessels: an application in microgravity. J. Tissue Culture Methods **14:**51–58.
33. **Stone, G., P. Wood, L. Dixon, M. Keyhan, and A. Matin.** 2002. Tetracycline rapidly reaches all the constituent cells of uropathogenic *Escherichia coli* biofilms. Antimicrob. Agents Chemother. **46:**2458–2461.
34. **Storrs-Mabilat, M.** 2001. Study of a microbial detection system for space applications. Second Workshop on Advanced Life Support, Noordwijk, The Netherlands.
35. **Tsao, Y. D., T. J. Goodwin, and D. A. Wolf.** 1992. Responses of gravity level variations in the NASA/JSC bioreactor system. Physiologist **35:**49–50.
36. **Waite, R. D., A. Papakonstantinopoulou, E. Littler, and M. A. Curtis.** 2005. Transcriptome analysis of *Pseudomonas aeruginosa* growth: comparison of gene expression in planktonic cultures and developing and mature biofilms. J. Bacteriol. **187:**6571–6576.
37. **Wilson, J. W., R. Ramamurthy, S. Porwollik, M. McClelland, T. Hammond, P. Allen, C. M. Ott, D. L. Pierson, and C. A. Nickerson.** 2002. Microarray analysis identifies *Salmonella* genes belonging to the low-shear modeled microgravity regulon. Proc. Natl. Acad. Sci. USA **99:**13807–13812.
38. **Wolf, D. A., and R. P. Schwartz.** 1991. Analysis of gravity-induced particle motion and fluid perfusion flow in the NASA-designed rotating zero-headspace tissue culture vessel. NASA Technical Paper 3143. NASA, Washington, D.C.
39. **Wolf, D. A., and R. P. Schwartz.** 1992. Experimental measurement of orbital paths of particles sedimenting within a rotating viscous fluid as influenced by gravity. NASA Technical Paper 3200. NASA, Washington, D.C.
40. **Zhao, Q., M. Jin, W. E. Muller, W. Zhang, X. Yu, and M. Deng.** 2003. Attachment of marine sponge cells of *Hymeniacidon perleve* on microcarriers. Biotechnol. Prog. **19:**1569–1573.